Analysis and numerics of the propagation speed for hyperbolic reaction-diffusion models

Corrado Lattanzio, Corrado Mascia, Ramón G. Plaza, Chiara Simeoni

Abstract This Chapter is divided into three Sections. The first one discusses different types of modeling reaction-diffusion phenomena, supporting the idea of the advantages of a description based on hyperbolic equations. Also, three basic numerical schemes are presented two of which can be applied for general hyperbolic systems, at the price of reduced performances when dealing with discontinuous initial data. The kind of underlying mechanism prescribes that, in the long-run, also these approaches are reliable. In the second Section, we focus on a class of 2×2 system corresponding to second order partial differential equations in one space dimension, adapted for simplified modeling of reaction-diffusion equations and focus on special traveling wave solutions, called propagating fronts. Special cases where the speed of propagation can be explicitly computed are also provided. In the third (and final) Section, we start with the presentation of the *phase-plane algorithm* which bears a reliable approximation of the propagation speed, assessing its validity in the case with damping where an explicit formula is available. Then, we propose two PDE-based algorithms to approximate the propagation speed, named *scout&spot algorithm* and the *LeVeque–Yee formula* and we attest their well-foundedness. We

Corrado Lattanzio
Dipartimento di Ingegneria e Scienze dell'Informazione e Matematica, Università degli Studi dell'Aquila, via Vetoio, Coppito I-67100, L'Aquila (Italy), e-mail: corrado@univaq.it

Corrado Mascia
Dipartimento di Matematica "Guido Castelnuovo", Sapienza Università di Roma, P.le Aldo Moro 2, I-00185 Roma (Italy), e-mail: corrado.mascia@uniroma1.it

Ramón G. Plaza
Instituto de Investigaciones en Matemáticas Aplicadas y en Sistemas, Universidad Nacional Autónoma de México, Circuito Escolar s/n C.P. 04510 Cd. de México (Mexico), e-mail: plaza@mym.iimas.unam.mx

Chiara Simeoni
Laboratoire J.A. Dieudonné UMR CNRS 7351, Université de Nice Sophia-Antipolis, Parc Valrose 06108 Nice Cedex 02 (France), e-mail: simeoni@unice.fr

conclude by suggesting the second one as more efficient tool in the determination of the velocity.

1 Models for reaction-diffusion phenomena

In this Section, we present different type of models useful for reaction-diffusion phenomena, supporting the idea that a description which makes use of hyperbolic equations is possible for both scalar equations and systems. The final Subsection presents three different numerical schemes which can be easily implemented in order to obtain reliable approximation of a reaction-diffusion model of hyperbolic type.

1.1 Diffusion is not always a parabolic mechanism

The standard approach to heat conduction in a homogeneous medium is based on the continuity relation linking the scalar unknown variable u with the vector-valued flux function $\mathbf{v}$, by means of the balance identity

$$\frac{d}{dt}\int_{\Omega} u(\mathbf{x},t)\,d\mathbf{x} + \int_{\partial\Omega} \mathbf{v}\cdot\mathbf{n}\,d\sigma = \int_{\Omega} f\,d\mathbf{x},$$

where Ω is an arbitrarily chosen control region with $d\mathbf{x}$ corresponding volume element, $\mathbf{n}$ is the outward normal to the smooth boundary $\partial\Omega$ with $d\sigma$ boundary element, and f is a volume contribution, to be considered, at first, as a given external constraint.

Applying Divergence Theorem, we can consider its localized version

$$\partial_t u + \mathrm{div}_{\mathbf{x}}\,\mathbf{v} = f, \tag{1}$$

where u and $\mathbf{v}$ describe respectively (heat) density and (heat) flux. The former is a scalar quantity; the latter is a vector with same dimension of the space variable $\mathbf{x}$.

To provide a closed system, equation (1) has to be coupled with some relation between u and $\mathbf{v}$. A frequent choice is the *Fourier's law*

$$\mathbf{v} = -a\,\mathrm{grad}_{\mathbf{x}}\,u \tag{2}$$

for some non-negative proportionality parameter a. Relation (2) is also called *Fick's law* when considered in bio-mathematical settings, *Ohm's law* in electromagnetism, and *Darcy's law* in porous media.

Coupling identity (1) with relation (2) gives raise to the balance law

$$\partial_t u = \mathrm{div}_{\mathbf{x}}\,(a\,\mathrm{grad}_{\mathbf{x}}\,u) + f. \tag{3}$$

The diffusion coefficient a may explicitly depend on space $\mathbf{x}$ and time t –as in the case of heterogeneous media– and also on the density variable itself u and its derivatives. Here, we focus mainly on the case $a > 0$.

While the continuity equation (1) can be considered reliable in general contexts, equation (2) should be regarded as a single possible choice among many others. In fact, quoting Lars Onsager (see [24]), Fourier's law is an approximate description of the process of conduction, which neglects the (short) relaxation time τ needed for acceleration. For practical purposes the time-lag can be neglected in all cases of heat conduction that are likely to be studied. Nevertheless, in many applications –among others, for dealing with biological tissues– extensions of the Fourier's law are required, with the specific aim of providing a more robust model, including in the picture both finite speed of propagation and inertial effects.

A first significant alternative to (2) is supported by the intuition that a delayed version should hold in place of the instantaneous response. The fact that the system requires a strictly positive amount of time τ to sense the gradient change translates into an identity of the *phase-lag relationship*

$$\mathbf{v}(\mathbf{x}, t+\tau) = -a \operatorname{grad}_{\mathbf{x}} u(\mathbf{x}, t).$$

Unfortunately, as proved in [14], the phase-lag model is ill-posed in the sense of Hadamard since it lacks of continuous dependence with respect to the initial data (see also [12]).

Surprisingly enough, well-posedness can be restored by truncating the Taylor's expansion for the unknown $\mathbf{v}$. Assuming τ to be small, we can consider the approximation

$$\begin{aligned} \mathbf{v}(\mathbf{x}, t+\tau) &= \mathbf{v}(\mathbf{x}, t) + \tau \partial_t \mathbf{v}(\mathbf{x}, t) + o(\tau) \\ &\approx \mathbf{v}(\mathbf{x}, t) + \tau\, \partial_t \mathbf{v}(\mathbf{x}, t), \end{aligned}$$

giving raise to the *Maxwell–Cattaneo's law*. Putting together with the balance law (1), we obtain the *(hyperbolic) reaction-diffusion system with relaxation*

$$\begin{cases} \partial_t u + \operatorname{div}_{\mathbf{x}} \mathbf{v} = f, \\ \tau \partial_t \mathbf{v} + a \operatorname{grad}_{\mathbf{x}} u = -\mathbf{v}. \end{cases} \tag{4}$$

The Maxwell–Cattaneo's law can be considered as a way for incorporating into the diffusion modelling some additional physical terms arising in the framework of Extended Irreversible Thermodynamics, [9, 15]. Such law, to be considered as a constitutive identity, has been originally proposed by Cattaneo [5, 6], following some pioneering intuition of James Clerk Maxwell (among others, let us quote [22, 23]). Sometimes, equation (4) is linked to Vernotte [25], and –more rarely– to Chester [7]. Extensions has been recently proposed in [8].

Eliminating the unknown $\mathbf{v}$ in the coupled system (1) and (4), we obtain the *one-field equation*, namely

$$\tau \partial_{tt} u + \partial_t \left(u - \tau f \right) = \operatorname{div}_{\mathbf{x}} \left(a \operatorname{grad}_{\mathbf{x}} u \right) + f. \tag{5}$$

The focal idea is that the balance between the flux $\mathbf{v}$ and the gradient $\mathrm{grad}_{\mathbf{x}} u$ of the density u is achieved only asymptotically in time, with decay described by the *relaxation time* $\tau > 0$. Such quantity can be regarded as the characteristic time for the crossover between ballistic motion and the onset of diffusion.

The Maxwell–Cattaneo's law furnishes the differential version of the delayed response to a change in the gradient $\mathrm{grad}_{\mathbf{x}} u$ as described by a memory kernel given by the exponential-rate law

$$\mathbf{v}(\mathbf{x},t) = \mathbf{v}_0(\mathbf{x}) e^{-t/\tau} - \frac{1}{\tau} \int_0^t e^{-(t-s)/\tau} a \, \mathrm{grad}_{\mathbf{x}} u(\mathbf{x},s)\, ds$$

which corresponds to the analogous formula in the context of viscoelasticity.

The main flaw is that equation (5) can violate the second law of thermodynamics, admitting scenarios where heat appear to be moving from cold to hot (see [16]). In this respect, correction to the notion of entropy have been proposed in order to partially solve the problem (for the case with no source term, see [11]).

An alternative approach is based on the postulation that the usual continuity equation (1) should be replaced by a delayed identity

$$\partial_t u(\mathbf{x}, t+\tau) + \mathrm{div}_{\mathbf{x}} \mathbf{v}(\mathbf{x},t) = f(\mathbf{x},t).$$

Truncating again the Taylor's expansion for u with respect to the second argument, we end up with

$$\tau \, \partial_{tt} u + \partial_t u + \mathrm{div}_{\mathbf{x}} \mathbf{v} = f. \tag{6}$$

Then, coupling with the standard Fourier's law (2), (6) gives the so-called *(hyperbolic) reaction-diffusion equation with damping*

$$\tau \, \partial_{tt} u + \partial_t u = \mathrm{div}_{\mathbf{x}} \left(a \, \mathrm{grad}_{\mathbf{x}} u \right) + f. \tag{7}$$

An alternative approach leading to a variation of (7) is proposed in [1]. In such a case, the hyperbolic equation is obtained by starting from space–time duality of a Minkowski space, and a simple Lorentz transformation, that are basic to the theory of special relativity. The starting point is an adapted version of the continuity equation, namely

$$\partial_t u + \mathrm{div}_{(t,\mathbf{x})} \mathbf{w} = f \qquad (\tau > 0),$$

where $\mathrm{div}_{(t,\mathbf{x})}$ is the scalar product of the operator $(i\sqrt{\tau}\,\partial_t, \partial_{x_1}, \ldots, \partial_{x_n})$ against the extended $(n+1)-$dimensional flux $\mathbf{w}$. Assuming the extended Fourier's relation

$$\mathbf{w} = -a \, \mathrm{grad}_{(t,\mathbf{x})} u,$$

where $\mathrm{grad}_{(t,\mathbf{x})} = (i\sqrt{\tau}\,\partial_t, \mathrm{grad}_{\mathbf{x}})$, we infer

$$\tau \partial_t (a \, \partial_t u) + \partial_t u = \mathrm{div}_{\mathbf{x}} (a \, \mathrm{grad}_{\mathbf{x}} u) + f,$$

which coincides with (7) when $a \equiv 1$.

However, the latter equation give rise to significant conceptual issues that makes the theory somewhat controversial. Among others, some quantities into play are described by complex numbers, with values involving imaginary "densities", which are hard to be interpreted.

Finally, let us determine an intermediate form somewhat in between (7) and (5). Let us denote by τ_1 and τ_2 the parameters for (6) and (4), respectively. Combining the delayed version of the continuity equation and the Maxwell–Cattaneo's law

$$\begin{cases} \tau_1 \partial_{tt} u + \partial_t u + \operatorname{div}_{\mathbf{x}} \mathbf{v} = f, \\ \tau_2 \partial_t \mathbf{v} + \mathbf{v} + a \operatorname{grad}_{\mathbf{x}} u = 0. \end{cases}$$

Differentiating the first equation with respect to t, taking the divergence with respect to $\mathbf{x}$ of the second equation and subtracting, we obtain the one-field equation for u

$$\tau_1 \tau_2 \partial_{ttt} u + (\tau_1 + \tau_2) \partial_{tt} u + \partial_t (u - \tau_2 f) = \operatorname{div}_{\mathbf{x}} (a \operatorname{grad}_{\mathbf{x}} u) + f.$$

Since the product $\tau_1 \tau_2$ is smaller with respect to the other 0-th/1-st order terms in τ_1 and τ_2 the third order time derivative can be disregarded (if bounded), thus giving raise to the hyperbolic equation

$$\tau \partial_{tt} u + \partial_t (u - \sigma f) = \operatorname{div}_{\mathbf{x}} (a \operatorname{grad}_{\mathbf{x}} u) + f.$$

where $\tau := \tau_1 + \tau_2$ and $\sigma := \tau_2$.

1.2 Reaction-diffusion by means of PDE systems

Passing to vector-valued density function $\mathbf{u} \in \mathbb{R}^p$, some modifications have to be taken into account. First of all, the vectorial form of the continuity equation becomes

$$\partial_t \mathbf{u} + \operatorname{Div}_{\mathbf{x}} \mathbf{V} = \mathbf{f}, \tag{8}$$

where Div denotes the divergence operator applied to each row of the matrix $\mathbf{V}$, and $\mathbf{f}$ is some vector-valued function.

Again, some additional relations coupling the dynamical variables u and $\mathbf{V}$ are required to close the system. As before, these could be of different nature. Denoting by $\operatorname{Grad}_{\mathbf{x}}$ the jacobian operator and having in mind the Fourier's law, we can conceive a relation of the following form

$$\begin{aligned} \mathbf{V} &= \text{linear functional applied to } \operatorname{Grad}_{\mathbf{x}} \mathbf{u} \\ &= -\mathbb{A} \operatorname{Grad}_{\mathbf{x}} \mathbf{u}. \end{aligned}$$

for some (4^{th}-order) tensor-valued function $\mathbb{A}$. Coupling with (8), the above identity gives the *(parabolic) reaction-diffusion system*

$$\partial_t \mathbf{u} = \mathrm{Div}_{\mathbf{x}} \left(\mathbb{A} \, \mathrm{Grad}_{\mathbf{x}} \mathbf{u} \right) + \mathbf{f}, \tag{9}$$

which can be regarded as the vectorial version of (3).

Considerations similar to the ones implemented in Subsection 1.1 support the search for alternatives to the Fourier's law, the first being the Maxwell–Cattaneo's law, which, in vectorial version, reads as

$$\tau \partial_t \mathbf{V} + \mathbf{V} = -\mathbb{A} \, \mathrm{Grad}_{\mathbf{x}} \mathbf{u}.$$

Of course, the latter equality can be generalized to the (more realistic) case in which any line of the flux matrix $\mathbf{V}$ has a different delay $\tau_1, \dots, \tau_p$. However, in what follows, we will concentrate on the case of a single time-scale τ for the sake of simplicity.

Coupling with the continuity equation (8), we end up with the *(hyperbolic) reaction-diffusion system with relaxation*

$$\begin{cases} \partial_t \mathbf{u} + \mathrm{Div}_{\mathbf{x}} \mathbf{V} = \mathbf{f}, \\ \tau \partial_t \mathbf{V} + \mathbb{A} \, \mathrm{Grad}_{\mathbf{x}} \mathbf{u} = -\mathbf{V}. \end{cases}$$

Differentiating by ∂_t the first equation, applying $\mathrm{Div}_{\mathbf{x}}$ to the second equation, and taking the difference, we deduce the *one-field system*

$$\tau \partial_{tt} \mathbf{u} + \partial_t \left(\mathbf{u} - \tau \mathbf{f} \right) = \mathrm{Div}_{\mathbf{x}} \left(\mathbb{A} \, \mathrm{Grad}_{\mathbf{x}} \mathbf{u} \right) + \mathbf{f}. \tag{10}$$

System (10) can be understood as the (hyperbolic) singular perturbation limit as $\tau \to 0^+$ of the (parabolic) system (9).

Alternatively, we can follow the strategy previously proposed considering a delayed continuity equality, which ends up in the *(hyperbolic) reaction-diffusion system with damping*

$$\tau \partial_{tt} \mathbf{u} + \partial_t \mathbf{u} = \mathrm{Div}_{\mathbf{x}} \big(\mathbb{A} \, \mathrm{Grad}_{\mathbf{x}} \mathbf{u} \big) + \mathbf{f}. \tag{11}$$

to be regarded as the vectorial version of (7).

In order to derive a sort of interpolation between (10) and (11), we follow the strategy proposed for (1.1), that is considering delays in both continuity identity and flux constitutive equality, with small relaxation times τ_1 and τ_2, so that the term with the product $\tau_1 \tau_2$ can be formally disregarded. In addition, restricting the attention to

$$\mathbb{A} = \text{constant} \qquad \text{and} \qquad \mathbf{f} = \mathbf{f}(\mathbf{u}),$$

we end up with the system

$$\tau \partial_{tt} \mathbf{u} + \partial_t \left\{ \mathbf{u} - \sigma \mathbf{f}(\mathbf{u}) \right\} = \mathrm{Div}_{\mathbf{x}} \left\{ \mathbb{A} \, \mathrm{Grad}_{\mathbf{x}} \mathbf{u} \right\} + \mathbf{f}(\mathbf{u}), \tag{12}$$

Later on, it will be transparent how the apparently harmless term $\sigma \mathrm{d}\mathbf{f}(\mathbf{u})$, negligible for σ small, may affect the dynamics and plays a crucial role in the long run.

In the class described by system (12), there are a some significant limiting regimes, with respect to the values of the parameters τ and $\sigma \in [0, \tau]$:

i. $\sigma = \tau = 0$ (undelayed continuity/undelayed flux):

$$\partial_t \mathbf{u} = \mathrm{Div}_{\mathbf{x}} \{\mathbb{A}\,\mathrm{Grad}_{\mathbf{x}} \mathbf{u}\} + \mathbf{f}(\mathbf{u});$$

ii. $\sigma = 0$, $\tau > 0$ (delayed continuity/undelayed flux):

$$\tau \partial_{tt} \mathbf{u} + \partial_t \mathbf{u} = \mathrm{Div}_{\mathbf{x}} \{\mathbb{A}\,\mathrm{Grad}_{\mathbf{x}} \mathbf{u}\} + \mathbf{f}(\mathbf{u});$$

iii. $\sigma = \tau > 0$ (undelayed continuity/delayed flux):

$$\tau \partial_{tt} \mathbf{u} + \partial_t \{\mathbf{u} - \tau \mathbf{f}(\mathbf{u})\} = \mathrm{Div}_{\mathbf{x}} \{\mathbb{A}\,\mathrm{Grad}_{\mathbf{x}} \mathbf{u}\} + \mathbf{f}(\mathbf{u}).$$

Additional specifications can be required on the zero-th order term $\mathbf{f}$ to add structure to the over-all system. In the scalar case, any continuous function f has a smooth primitive, producing a corresponding potential W (more details on such a case, will be provided later on). Differently, when the dimension is strictly greater than 1, additional constraints are needed in order to make this requirement to be satisfied. Specifically, for smooth functions, a necessary condition for the existence of a *potential function* W such that

$$\mathrm{grad}_{\mathbf{u}} W(\mathbf{u}) = -\mathbf{f}(\mathbf{u}), \tag{13}$$

is demanding that the jacobian matrix $\mathrm{d}\mathbf{f}$ of $\mathbf{f}$ is symmetric, that is

$$\mathrm{d}\mathbf{f}(\mathbf{u})^{\top} = \mathrm{d}\mathbf{f}(\mathbf{u}). \tag{14}$$

Such condition is sufficient if the domain is simply connected or star-shaped.

Incidentally, let us observe that, assuming the symmetry condition (14), system (12) is endowed with a natural *Lyapunov functional*, i.e. a global function which is not-increasing along any given trajectory. To simplify the formalism, we concentrate on the one-dimensional spatial case, limiting ourselves to

$$\tau \partial_{tt} \mathbf{u} + \partial_t \{\mathbf{u} - \sigma \mathbf{f}(\mathbf{u})\} = \mathbf{A}\, \partial_{xx} \mathbf{u} + \mathbf{f}(\mathbf{u}), \tag{15}$$

For $\tau = \sigma = 0$, we obtain the standard parabolic reaction-diffusion system

$$\partial_t \mathbf{u} = \mathbf{A}\, \partial_x^2 \mathbf{u} + \mathbf{f}(\mathbf{u})$$

Property (13) –or (14)– guarantees the presence of a *variational structure*. Specifically, the functional $\mathscr{E}_0$ defined by

$$\mathscr{E}_0[\mathbf{u}] := \int_{\mathbb{R}} \Big\{ \tfrac{1}{2} \mathbf{A} \partial_x \mathbf{u} \cdot \partial_x \mathbf{u} + W(\mathbf{u}) \Big\} dx,$$

together with some appropriate integrability conditions at $\pm\infty$, is a Lyapunov functional for the system (15). Indeed, there holds

$$\frac{d}{dt} \mathscr{E}_0[\mathbf{u}] + \int_{\mathbb{R}} |\partial_t \mathbf{u}|^2 \, dx = 0,$$

exhibiting a *dissipative property* for $\mathscr{E}_0$.

Similar considerations can be done also in the case (15), giving raise to a differential equality for the *modified energy*

$$\mathscr{E}_\tau[\mathbf{u}] := \tfrac{1}{2}\tau|\partial_t \mathbf{u}|^2 + \mathscr{E}_0[\mathbf{u}].$$

Then, setting $\mathbf{Q}_\sigma := \mathbf{I} - \sigma \mathrm{d}\mathbf{f}(\mathbf{u})$, there holds

$$\frac{d}{dt}\mathscr{E}_\tau[\mathbf{u}] + \int_{\mathbb{R}} \mathbf{Q}_\sigma \partial_t \mathbf{u} \cdot \partial_t \mathbf{u}\, dx = 0.$$

Again, choosing $\sigma \geq 0$ so that $\mathbf{Q}_\sigma > 0$, dissipation is transparent.

1.3 Three basic numerical schemes in one space dimension

For $\mathbf{u} \in \mathbb{R}^p$ and in one space dimension, the tensor $\mathbb{A}$ reduces now to a $p \times p$ matrix $\mathbf{A}$, that is $\mathbb{A} = \mathbf{A} = (a^{i1}_{1\ell})$ since two of the four indeces are now fixed and equal to 1. For the sake of simplicity, we limit ourselves to the case $\mathbf{A} = a\mathbf{I}$ for some $a > 0$. Hence, we consider the system in one space-dimension

$$\tau \partial_{tt}\mathbf{u} + \partial_t \left\{\mathbf{u} - \sigma \mathbf{f}(\mathbf{u})\right\} = a\partial_{xx}\mathbf{u} + \mathbf{f}(\mathbf{u}). \tag{16}$$

First-order reduction algorithm

System (16) has an immediate numerical description, obtained by rewriting it in first-order form as

$$\begin{cases} \partial_t \mathbf{u} = \mathbf{v}, \\ \tau\, \partial_t \mathbf{v} = a\, \partial_{xx}\mathbf{u} + \mathbf{f}(\mathbf{u}) - \{\mathbf{I} - \sigma\, \mathrm{d}\mathbf{f}(\mathbf{u})\}\, \mathbf{v}. \end{cases} \tag{17}$$

Firstly, we discretize the spatial part, introducing a uniform mesh with uniform step dx, obtaining

$$\begin{cases} \dfrac{d\mathbf{u}_j}{dt} = \mathbf{v}_j \\ \tau \dfrac{d\mathbf{v}_j}{dt} = \dfrac{a}{\mathrm{dx}^2}\left(\mathbf{u}_{j+1} - 2\mathbf{u}_j + \mathbf{u}_{j-1}\right) + \mathbf{f}(\mathbf{u}_j) - \left\{\mathbf{I} - \sigma\, \mathrm{d}\mathbf{f}(\mathbf{u}_j)\right\}\mathbf{v}_j \end{cases} \tag{18}$$

As a second step, we have to discretize with respect to the time variable. In order to perform such a step, there are many different choices.

To start with, we choose an implicit-explicit scheme (IMEX), limiting the implicit description to the linear part of the system, so that

$$\begin{cases} \dfrac{\mathbf{u}_j^{n+1}-\mathbf{u}_j^n}{\mathrm{dt}} = \mathbf{v}_j^{n+1} \\ \tau\dfrac{\mathbf{v}_j^{n+1}-\mathbf{v}_j^n}{\mathrm{dt}} = \dfrac{a}{\mathrm{dx}^2}\left(\mathbf{u}_{j+1}^{n+1}-2\mathbf{u}_j^{n+1}+\mathbf{u}_{j-1}^{n+1}\right)+\mathbf{f}(\mathbf{u}_j^n)-\mathbf{v}_j^{n+1}+\sigma\mathrm{d}\mathbf{f}(\mathbf{u}_j^n)\mathbf{v}_j^n \end{cases}$$

which gives the *first-order reduction algorithm*

$$\begin{cases} \mathbf{u}_j^{n+1}-\mathrm{dt}\,\mathbf{v}_j^{n+1} = \mathbf{u}_j^n \\ \alpha\left(-\mathbf{u}_{j+1}^{n+1}+2\mathbf{u}_j^{n+1}-\mathbf{u}_{j-1}^{n+1}\right)+(1+\beta)\,\mathbf{v}_j^{n+1} = \mathbf{v}_j^n+\beta\,\mathbf{f}(\mathbf{u}_j^n) \\ \qquad\qquad +\sigma\beta\,\mathrm{d}\mathbf{f}(\mathbf{u}_j^n)\mathbf{v}_j^n, \end{cases} \tag{19}$$

where $\alpha := a\,\mathrm{dt}/\tau\mathrm{dx}^2$, $\beta := \mathrm{dt}/\tau$. Solving such an implicit-explicit algorithm furnishes the numerical approximation of the real solution

$$\begin{pmatrix}\mathbf{u}^{n+1}\\ \mathbf{v}^{n+1}\end{pmatrix} = \mathbf{A}^{-1}\begin{pmatrix}\mathbf{u}^n\\ \mathbf{v}^n+\beta\,\mathbf{f}(\mathbf{u}^n)+\sigma\beta\,\mathrm{d}\mathbf{f}(\mathbf{u}^n)\mathbf{v}^n\,\mathrm{dt}\end{pmatrix}$$

where $\mathbf{A}$ describes the coefficients of the left-hand side matrix in (19).

Liénard-type algorithm

A second type of algorithm is inspired by the so-called "Liénard second order equation" which is

$$\tau\frac{d^2u}{dt^2}+g(u)\frac{du}{dt}+h(u)=0.$$

for some given functions g and h. In such a case, the above equation can be rewritten as a first order system by setting

$$\tau\frac{du}{dt} = v-G(u), \qquad \frac{dv}{dt} = -h(u)$$

where G is a primitive of the function g. Applied to system (16), let us consider an algorithm based on the decomposition of the system given by

$$\begin{cases} \tau\partial_t\mathbf{u} = \mathbf{v}-\mathbf{u}+\sigma\mathbf{f}(\mathbf{u}), \\ \partial_t\mathbf{v} = a\,\partial_{xx}\mathbf{u}+\mathbf{f}(\mathbf{u}). \end{cases} \tag{20}$$

In what follows, we refer to such an approach a *Liénard-type algorithm*.

As before, discretizing the spatial part with respect to an uniform mesh with step dx, we infer

$$\begin{cases} \tau\dfrac{d\mathbf{u}_j}{dt} = \sigma\mathbf{f}(\mathbf{u}_j)-\mathbf{u}_j+\mathbf{v}_j \\ \dfrac{d\mathbf{v}_j}{dt} = \dfrac{a}{\mathrm{dx}^2}\left(\mathbf{u}_{j+1}-2\mathbf{u}_j+\mathbf{u}_{j-1}\right)+\mathbf{f}(\mathbf{u}_j). \end{cases} \tag{21}$$

Let us observe that, at the continuous level, systems (17) and (20), and at semi-discretized algorithm, systems (18) and (21), are completely equivalent, the difference being only in the choice of the variable $\mathbf{v}$.

The crucial difference emerges in the subsequent step, where the time discretization is taken into account and the difference between linear (implicit) vs nonlinear (explicit) discretizations. On top of that, let us also incidentally observe that the Liénard-type algorithm does not require an explicit computation of the jacobian matrix $\mathrm{d}\mathbf{f}$ at the value $\mathbf{u}_j^n$.

Proceeding in the spirit of what we have done before, we infer

$$\begin{cases} \tau \dfrac{\mathbf{u}_j^{n+1}-\mathbf{u}_j^n}{\mathrm{dt}} = \sigma \mathbf{f}(\mathbf{u}_j^n) - \mathbf{u}_j^{n+1} + \mathbf{v}_j^{n+1} \\ \dfrac{\mathbf{v}_j^{n+1}-\mathbf{v}_j^n}{\mathrm{dt}} = \dfrac{a}{\mathrm{dx}^2}\left(\mathbf{u}_{j+1}^{n+1} - 2\mathbf{u}_j^{n+1} + \mathbf{u}_{j-1}^{n+1}\right) + \mathbf{f}(\mathbf{u}_j^n) \end{cases}$$

from which we obtain the IMEX linear system

$$\begin{cases} (1+\beta)\mathbf{u}_j^{n+1} - \beta \mathbf{v}_j^{n+1} = \mathbf{u}_j^n + \beta\sigma \mathbf{f}(\mathbf{u}_j^n) \\ \alpha\left(-\mathbf{u}_{j+1}^{n+1} + 2\mathbf{u}_j^{n+1} - \mathbf{u}_{j-1}^{n+1}\right) + \mathbf{v}_j^{n+1} = \mathbf{v}_j^n + \mathbf{f}(\mathbf{u}_j^n)\mathrm{dt} \end{cases} \tag{22}$$

with $\alpha := a\mathrm{dt}/\mathrm{dx}^2$ and $\beta := \mathrm{dt}/\tau$. The solution of such an iteration provides the numerical approximation of the solution $(\mathbf{u},\mathbf{v})$

$$\begin{pmatrix} \mathbf{u}^{n+1} \\ \mathbf{v}^{n+1} \end{pmatrix} = \mathbf{A}^{-1} \begin{pmatrix} \mathbf{u}_j^n + \beta\sigma\mathbf{f}(\mathbf{u}_j^n) \\ \mathbf{v}_j^n + \mathbf{f}(\mathbf{u}_j^n)\mathrm{dt} \end{pmatrix}$$

where $\mathbf{A}$ describes the coefficients of the left-hand side matrix in (22).

Kinetic algorithm

A third viable algorithm is limited to the case $\sigma = \tau > 0$. In such a situation, it is possible to start back from the derivation of the model, i.e. the coupling of the balance law together with the Maxwell–Cattaneo's relation,

$$\partial_t \mathbf{u} + \partial_x \mathbf{v} = \mathbf{f}(\mathbf{u}), \qquad \tau\,\partial_t \mathbf{v} + \mathbf{v} = -a\,\partial_x \mathbf{u}.$$

Here, τ and a can be considered as diagonal matrices with elements $(\tau_1,\dots,\tau_n)$ and $(a_1,\dots,a_n)$, which are here considered possibly different one from the other. Therefore, we end up with the system

$$\begin{cases} \partial_t u_i + \partial_x v_i = f_i(u_1,\dots,u_n), \\ \tau_i\,\partial_t v_i + a_i\,\partial_x u_i = -v_i. \end{cases} \tag{23}$$

The coupling is due to the presence in the first equation of the term $\mathbf{f} = (f_1,\dots,f_n)$. Differently, the second equation in (23) involves only the components u_i and v_i.

The coefficients of the principal part of the differential operator in (23) are described by the block-diagonal matrix $\mathbf{A} = \text{blockdiag}(\mathbf{A}_1, \dots, \mathbf{A}_n)$ with

$$\mathbf{A}_i := \begin{pmatrix} 0 & 1 \\ a_i/\tau_i & 0 \end{pmatrix} \qquad i = 1, \dots, n.$$

Thus, the eigenvalues of the $2n \times 2n$ matrix $\mathbf{A}$, given by the roots of the polynomial

$$p(\lambda) = \det(\mathbf{A} - \lambda \mathbf{I}) = \prod_{i=1}^{n} \left(\lambda^2 - \rho_i^2\right),$$

where $\rho_i := \sqrt{a_i/\tau_i}$, are $\lambda = \pm\rho_i$ for $i = 1, \dots, n$.

Introducing the diagonal variables $(\mathbf{r}, \mathbf{s}) = (r_1, \dots, r_n, s_1, \dots, s_n)$, defined by

$$r_i := \frac{1}{2}\left(u_i - \frac{v_i}{\rho_i}\right), \qquad s_i := \frac{1}{2}\left(u_i + \frac{v_i}{\rho_i}\right),$$

the system (23) becomes

$$\begin{cases} \partial_t r_i - \rho_i \partial_x r_i = \dfrac{1}{2\tau_i}(-r_i + s_i) + \dfrac{1}{2} f_i(r_1 + s_1, \dots, r_n + s_n), \\ \partial_t s_i + \rho_i \partial_x s_i = \dfrac{1}{2\tau_i}(+r_i - s_i) + \dfrac{1}{2} f_i(r_1 + s_1, \dots, r_n + s_n). \end{cases}$$

As before, we firstly consider a discretization of the spatial part with a uniform mesh described by the step dx, and taking into account the up-wind nature of the model; we, thus, obtain

$$\begin{cases} \dfrac{dr_{i,j}}{dt} - \rho_i \dfrac{r_{i,j+1} - r_{i,j}}{\mathrm{dx}} + \dfrac{1}{2\tau_i}(+r_{i,j} - s_{i,j}) = \dfrac{1}{2} f_i(r_1 + s_1, \dots, r_n + s_n), \\ \dfrac{ds_{i,j}}{dt} + \rho_i \dfrac{s_{i,j} - s_{i,j-1}}{\mathrm{dx}} + \dfrac{1}{2\tau_i}(-r_{i,j} + s_{i,j}) = \dfrac{1}{2} f_i(r_1 + s_1, \dots, r_n + s_n). \end{cases}$$

Next, we follow the same strategy of the IMEX algorithm, that is we discretize implicitly only the linear part of the system. Thus, we infer

$$\begin{cases} \dfrac{r_{i,j}^{n+1} - r_{i,j}^{n}}{\mathrm{dt}} - \dfrac{\rho}{\mathrm{dx}}\left(r_{i,j+1}^{n+1} - r_{i,j}^{n+1}\right) - \dfrac{1}{2\tau_i}\left(-r_{i,j}^{n+1} + s_{i,j}^{n+1}\right) = \dfrac{1}{2} f_i(\mathbf{r}^n + \mathbf{s}^n), \\ \dfrac{s_{i,j}^{n+1} - s_{i,j}^{n}}{\mathrm{dt}} + \dfrac{\rho}{\mathrm{dx}}\left(s_{i,j}^{n+1} - s_{i,j-1}^{n+1}\right) - \dfrac{1}{2\tau_i}\left(r_{i,j}^{n+1} - s_{i,j}^{n+1}\right) = \dfrac{1}{2} f_i(\mathbf{r}^n + \mathbf{s}^n), \end{cases}$$

that gives

$$\begin{cases} (1 + \alpha_i + \beta_i)\, r_{i,j}^{n+1} - \alpha_i r_{i,j+1}^{n+1} - \beta_i s_{i,j}^{n+1} = r_{i,j}^{n} + \dfrac{1}{2} f_i(\mathbf{r}^n + \mathbf{s}^n)\, \mathrm{dt}, \\ -\beta_i r_{i,j}^{n+1} - \alpha_i s_{i,j-1}^{n+1} + (1 + \alpha_i + \beta_i)\, s_{i,j}^{n+1} = s_{i,j}^{n} + \dfrac{1}{2} f_i(\mathbf{r}^n + \mathbf{s}^n)\, \mathrm{dt}, \end{cases}$$

where $\alpha_i = \rho_i \, \mathrm{dt}/\mathrm{dx}$, $\beta_i = \mathrm{dt}/2\tau_i$.

Again, denoting by $\mathbf{A}$ the coefficients' matrix of the couple $(\mathbf{r},\mathbf{s})$ in the above system, we obtain the iteration formula

$$\begin{pmatrix} \mathbf{r}^{n+1} \\ \mathbf{s}^{n+1} \end{pmatrix} = \mathbf{A}^{-1} \begin{pmatrix} \mathbf{r}^n + \mathbf{f}(\mathbf{r}^n + \mathbf{s}^n)\,\mathrm{dt}/2 \\ \mathbf{s}^n + \mathbf{f}(\mathbf{r}^n + \mathbf{s}^n)\,\mathrm{dt}/2 \end{pmatrix}.$$

2 Some waves are better than others

We start this Section by presenting traveling wave solutions, which are supported by hyperbolic reaction-diffusion system, using, as a prototypes, the case of monostable and bistable reaction terms. Next, we focus on a special class of waves, called *propagation fronts* explored in details in the case of a bistable reaction term. Special cases where the speed of propagation can be explicitly computed are also provided.

2.1 Traveling waves

Among the infinitely many solutions of a partial differential equations, some solutions exhibits an augmented "stability", due to the fact that they possess an additional amount of internal symmetry. A recurrent type of such kind of solutions are the so-called *traveling waves* (with planar symmetry), i.e. solutions of the form

$$\mathbf{u}(\mathbf{x},t) := \phi(\mathbf{k}\cdot\mathbf{x} - c\,t) \tag{24}$$

for some unitary vector $\mathbf{k}$. Here ϕ is called the *profile of the wave* and c its *propagation speed*.

For such kind of solutions, PDEs are reduced to ODEs, whose unknowns depend on the scalar variable $\xi := \mathbf{k}\cdot\mathbf{x} - c\,t$ with the value c to be determined together with the function ϕ. As an example, inserting the ansatz (24) in (12) and noticing that

$$\mathrm{Grad}_{\mathbf{x}}\mathbf{u} = \frac{d\phi}{d\xi} \otimes \mathbf{k},$$

$$\mathrm{Div}_{\mathbf{x}} \left\{ \mathbb{A} \left(\frac{d\phi}{d\xi} \otimes \mathbf{k} \right) \right\} = \mathbb{A}\,\mathrm{Div}_{\mathbf{x}} \left(\frac{d\phi}{d\xi} \otimes \mathbf{k} \right) = \mathbb{A} \left(\frac{d^2\phi}{d\xi^2} \otimes \mathbf{k} \right),$$

we end up with an ODE for the profile ϕ, parametrized by the velocity c,

$$\mathbb{A} \left(\frac{d^2\phi}{d\xi^2} \otimes \mathbf{k} \right) + c^2\tau \frac{d^2\phi}{d\xi^2} + c\,\{\mathbf{I} - \sigma d\mathbf{f}(\phi)\} \frac{d\phi}{d\xi} + \mathbf{f}(\phi) = 0,$$

Since the above system is autonomous, the profile is determined up to translations. This implies that the translation $\phi_\delta := \phi(\cdot - \delta)$ with $\delta \in \mathbb{R}$ of a given traveling

wave $\phi = \phi(\cdot)$ is itself a traveling wave solution for the same system. Such properties have an immediate consequence: the derivative of ϕ with respect to its argument is an eigenfunction for the corresponding linearized operator at ϕ relative to the eigenvalue $\lambda = 0$. This influences the stability properties of the wave, dictating the fact that, at most, *orbital stability* could be expected, meaning convergence of (small) perturbations to the manifold $\{\phi_\delta : \delta \in \mathbb{R}\}$. Presence/absence of an *asymptotic phase*, viz. convergence to a definite element of the manifold, is the (natural) subsequent issue.

Depending on specific properties of the profile function ϕ, different names are associated to traveling waves:

i. if ϕ converges to some asymptotic states $\phi_\pm$ (which are necessarily two distinct equilibria of the model) with $\phi_- \neq \phi_+$, the solution is called a *front*;
ii. if ϕ converges to the same asymptotic state $\overline{\phi}$ (which is necessarily an equilibrium of the model), the solution is said to be a *pulse*;
iii. if ϕ is periodic, the solution is a *wave-train*.

In the state space, the three configurations correspond, respectively, to the presence of a heteroclinic orbit, a homoclinic orbit or a cycle. From now on, we focus on fronts; also, we restrict the attention to the spatial one-dimensional case.

A further reduction concerns with the size of the vector $\mathbf{u}$ which is, from the time being, regarded as a scalar quantity (and denoted by u), thus restricting the attention to the second-order scalar equation

$$\tau\,\partial_{tt}u + \partial_t\{u - \sigma f(u)\} = a\,\partial_{xx}u + f(u). \tag{25}$$

where f is an appropriate functions and τ, σ, a are positive constants.

Monostable and bistable nonlinearities

Following [2, 3] (and descendants), we select here two types of nonlinearities.

i. *Monostable.* The function f is assumed to be smooth, strictly positive in some fixed interval $(0,1)$, negative in $(-\infty,0)\cup(1,+\infty)$, with simple zeros;
ii. *Bistable.* The function f is assumed to be smooth, strictly positive in some fixed interval $(-\infty,0)\cup(\alpha,1)$, negative in $(0,\alpha)\cup(1,+\infty)$, with simple zeros.

In both situations, we introduce the corresponding potential

$$W(u) := -\int_0^u f(s)\,ds$$

The function W is decreasing for the monostable regime and it has a double-well form for the bistable one.

The former case, whose prototype is $f(u) \propto u(1-u)$, corresponds to a logistic-type reaction term and it is usually referred to as *Fisher–KPP equation* (using the initials of the names Kolmogorov, Petrovskii and Piscounov). The potential corresponding to $f(u) = \kappa u(1-u)$ is

$$W(u) = \tfrac{1}{6}\kappa\left(-3u^2 + 2u^3\right),$$

drawn in Figure 1 (continuous line). Different kind of monostable reaction function

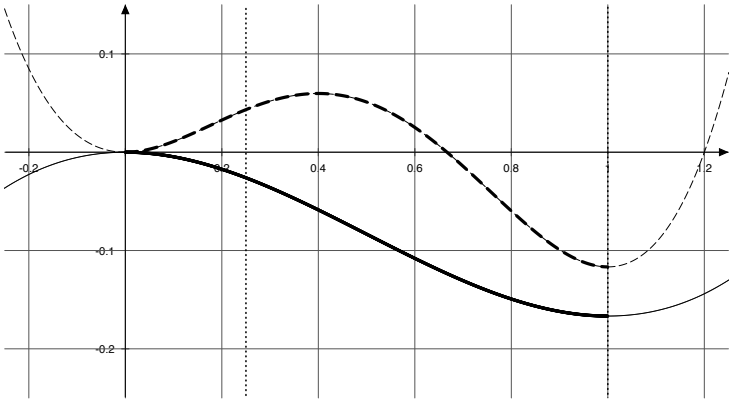

Fig. 1 The potentials W relative to the functions $f(u) = u(1-u)$ (monostable, continuous) and $f(u) = \kappa u(1-u)(u-\alpha)$ with $\kappa = 7$ and $\alpha = 0.4$ (bistable, dashed).

f are the *Gompertz term*, i.e. $f(u) = \kappa u \ln u$, and *von Bertalanffy term*, i.e. $f(u) = \kappa(u^\mu - u)$ with $\mu \in (0,1)$, corresponding potentials being $W(u) = \kappa u^2(2\ln|u| - 1)/4$ and $W(u) = \kappa\left\{u^2/2 - u^{\mu+1}/(\mu+1)\right\}$, respectively. The main difference is in the location of the tangent line at $u = 0$ which is vertical in the last two cases and it playes a crucial role in the statement of existence of propagating fronts.

The latter, whose behaviour is roughly given by the third order polynomial $f(u) \propto u(u-\alpha)(1-u)$ with $\alpha \in (0,1)$, is called *Allen–Cahn equation* (sometimes, also bear the names of *Nagumo* and/or *Ginzburg–Landau*). The potential which corresponds to $f(u) = u(u-\alpha)(1-u)$ is

$$W(u) = \tfrac{1}{12}\kappa\left\{6\alpha u^2 - 4(1+\alpha)u^3 + 3u^4\right\}. \tag{26}$$

The presence of the additional intermediate zero of the function f given by α emerged in ecological context where it describes the so-called *Allee-type effect*, needed in situation where some cooperation is required for survival (see [10] for a detailed description of the topic).

2.2 Propagating fronts

Both monostable and bistable nolinearities share a common crucial feature: they support existence of heteroclinic traveling waves.

Definition 1. A *propagating front* is a traveling wave solution for a given PDE system having the special form $u(x,t) = \phi(\xi)$ where $\xi := x - ct$, connecting two different asymptotic states $\phi(\pm\infty) = \phi_\pm$ with $\phi_- \neq \phi_+$.

In what follows, we assume for definiteness $\phi_- = 1$ and $\phi_+ = 0$.

The main goal stems in showing existence of a heteroclinic solution to the corresponding second order differential equation

$$(a - \tau c^2)\frac{d^2\phi}{d\xi^2} + c\frac{d}{d\xi}\left\{\phi + \sigma\frac{dW}{du}(\phi)\right\} - \frac{dW}{du}(\phi) = 0, \tag{27}$$

with boundary conditions $\phi(-\infty) = 1$, $\phi(+\infty) = 0$. Equivalentlly, the second order differential equation (27) can be rewritten as

$$\begin{cases} \dfrac{d\phi}{d\xi} = \psi, \\ \dfrac{d\psi}{d\xi} = \dfrac{1}{a - \tau c^2}\left\{\dfrac{dW}{du}(\phi) - c\left[1 + \sigma\,\dfrac{d^2W}{du^2}(\phi)\right]\psi\right\} \end{cases}$$

Next, assume $1 + \sigma W''(s) > 0$ for any s under consideration. Multiplying equation (27) by $d\phi/d\xi$, we deduce the identity

$$\frac{d}{d\xi}\left\{\tfrac{1}{2}(a - \tau c^2)\left(\frac{d\phi}{d\xi}\right)^2 - W(\phi)\right\} + c\left(1 + \sigma W''\right)\left(\frac{d\phi}{d\xi}\right)^2 = 0.$$

Thus, integrating in $\mathbb{R}$, we infer

$$c = \frac{W(0) - W(1)}{\int_{\mathbb{R}}\left(1 + \sigma W''\right)(\phi')^2\,dx} \tag{28}$$

From this relation, it is readily observed that the speed c is strictly positive if and only if $W(1) < W(0)$. In particular, in the monostable case, $\phi_- = 0$ is a maximum point and $\phi_+ = 1$ is a minimum for W and thus c is strictly positive. Differently, in the bistable case, W is a double-well potential and thus the speed is positive or negative depending on the depth difference of the two wells $W(0) - W(1)$.

The starting point in proving existence of propagation fronts is the stability analysis of the singular points of (27), i.e. constant values $\bar{u}$ with the property $f(\bar{u}) = 0$, with respect to the ordinary differential system obtained by considering the traveling wave ansatz where the speed c is, for the moment, an external parameter.

Linearizing at $\bar{u}$ the second order differential equation (27), we infer

$$\begin{cases} \dfrac{d\phi}{d\xi} = \psi, \\ \dfrac{d\psi}{d\xi} = \dfrac{1}{a - \tau c^2}\left\{W''(\bar{u})\,\phi - c\left\{1 + \sigma W''(\bar{u})\right\}\psi\right\}. \end{cases} \tag{29}$$

The characteristic polynomial is

$$p(\lambda;\bar{u},c) := \frac{1}{(a-\tau c^2)}\left\{(a-\tau c^2)\lambda^2 + c\left(1+\sigma W''(\bar{u})\right)\lambda - W''(\bar{u})\right\}; \tag{30}$$

thus, setting

$$\Delta(\bar{u},c) := c^2\left\{1+\sigma W''(\bar{u})\right\}^2 + 4(a-\tau c^2)W''(\bar{u}) > 0, \tag{31}$$

the two roots of $p = p(\cdot;\bar{u},c)$ are

$$\lambda_\pm(\bar{u},c) = \frac{-c\,(1+\sigma W''(\bar{u})) \pm \sqrt{\Delta(\bar{u},c)}}{2(a-\tau c^2)}. \tag{32}$$

Since they have opposite signs if $W''(\bar{u}) > 0$, the singular point $(\bar{u},0)$ is a saddle point for (29).

Differently, if $W''(\bar{u}) < 0$ (hence $\bar{u}$ is unstable with respect to the PDE), the two roots are either complex conjugates or both real with the same sign, thus they define either a spiral or a node. Assuming $1+\sigma W''(\bar{u}) > 0$, the spiral and the node are stable (or unstable, respectively) if $c > 0$ (or $c < 0$, resp.).

Hence, the heteroclinic orbit is a node/saddle connection in the case of Fisher–KPP equation (monostable case) and a saddle/saddle connection in the case of the Allen–Cahn equation (bistable case) for both the parabolic, obtained with the choice $\tau = 0$, and the hyperbolic equations, given by $\tau > 0$, having a specific relevant consequence in term of the multiplicity of the speeds.

To fix idea, let us give a closer look to traveling waves with a monotone decreasing profile, that is $\phi_- := 1 > 0 =: \phi_+$. The opposite case can be deduced by straightforward symmetry arguments. For the node/saddle connection, the situation is rather complicated; while in the case of the saddle/saddle connection, the picture is somewhat easier.

In the former case, we have to restrict the attention to the regimes of the parameter c such that the critical point is an unstable node, hence, ruling out (stable and unstable) spirals and stable nodes. As well-known, for $W''(\bar{u}) < 0$, there is a specific parameter Δ discriminating whether the two roots of the polynomial p are real or not. When Δ, given in (31), is strictly positive it guarantees that such roots are real and distinct: recalling the request $\sigma \in [0,\tau]$, positivity is readily checked. Next, we search for intersection between the two-dimensional unstable manifold of the critical point $\phi_- = 1$ at $-\infty$ and the one-dimensional stable manifold at $\phi_+ = 0$ at $+\infty$. In term of dimensions, the situation is favourable and, thus, existence could be provided for a whole half-line of values for the parameter c. For more details on the monostable case, we refer to [13] in the parabolic case (i.e. $\sigma = \tau = 0$) and to [4] for the case $\sigma = \tau > 0$.

In the latter case, the one-dimensional manifold of the steady state $\phi_- = 1$ has to intersect at some point the stable manifold of the steady state $\phi_+ = 0$. Being the system planar, the corresponding stable and unstable manifolds are one-dimensional and thus the intersection of the two manifolds is non-generic, corresponding to the

fact that the speed c has to be appropriately tuned. This translates into the existence of a specific value of the speed for which the heteroclinic connection emerges.

From now on, we restrict the attention to the bistable case with $W(1) \leq W(0)$ so that $c \geq 0$, with the exception of some minor deviations from the mainstream dedicated to the monostable case. In particular, we may restrict the attention to the sub-characteristic case $a - \tau c^2 > 0$.

Introducing the variable $\zeta = \xi / \sqrt{a - \tau c^2}$, equation (27) becomes simpler, namely

$$\frac{d^2\phi}{d\zeta^2} + \gamma \frac{d}{d\zeta} \left\{ \phi + \sigma W'(\phi) \right\} - W'(\phi) = 0, \tag{33}$$

where

$$c_\tau := \frac{c}{\sqrt{a - \tau c^2}}. \tag{34}$$

Equation (33) can be equivalently rewritten as the first order system

$$\begin{cases} \dfrac{d\phi}{d\zeta} = \psi, \\ \dfrac{d\psi}{d\zeta} = W'(\phi) - c_\tau \left(1 + \sigma W''(\phi)\right) \psi \end{cases} \tag{35}$$

with asymptotic conditions $(\phi, \psi)(-\infty) = (1, 0)$ and $(\phi, \psi)(+\infty) = (0, 0)$. A different first order form for (33) is given by the Liénard form

$$\begin{cases} \dfrac{d\phi}{d\zeta} = -c_\tau \left\{ \phi + \sigma W'(\phi) \right\} + \chi, \\ \dfrac{d\chi}{d\zeta} = W'(\phi), \end{cases} \tag{36}$$

with asymptotic conditions $(\phi, \chi)(-\infty) = (1, 0)$ and $(\phi, \chi)(+\infty) = (0, 0)$.

Such simplified form for the equation (27) is particularly convenient when passing from local to global analysis, using the *rotated vector field property* of system (33). The final statement relative to existence of propagating front is reported here, for readers' convenience, as taken from [19].

Theorem 1. *Let W be a double-well potential with local minima at 0 and 1. If $\tau > 0$, $\sigma \in [0, \tau]$ and $1 + \sigma W''(s) > 0$ for any $s \in [0, 1]$, then there exists a unique value $c_* \in \mathbb{R}$ such that the equation (27) has a monotone increasing solution ϕ with asymptotic states $\phi(-\infty) = 1$ and $\phi(+\infty) = 0$.*

2.3 Special cases with explicit propagation speeds

Next, we focus on three special cases for which an explicit formula is available. The first one concerns with the case of two wells of equal depth. Next, we pass to

consider the specific case of a third order polynomial reaction term for which explicit formulas for both the standard parabolic equation and the hyperbolic equation with damping can be determined. Finally, we discuss the case of a piecewise linear reaction function with a jump located at the intermediate value α.

Two wells of equal depth

The case of a double-well potential W with wells of equal depth can be treated separately, since (28) indicates that $c_\star = 0$, indipendently on the values of $\sigma \geq 0$.

Proposition 1. *Let $\tau \geq 0$ and $\sigma \in [0,\tau]$. In addition, let $f = -W'$ with W double-well potential having wells located at 0 and 1 with $W(0) = W(1)$. Then, equation* (25) *supports monotone steady states connecting equilibria $\phi_- = 1$ and $\phi_+ = 0$.*

Proof. We report here the standard proof for reader's convenience. Substituting $c = 0$, equation (27) reduces to the equation

$$a\frac{d^2\phi}{d\xi^2} - W'(\phi) = 0,$$

Multiplying by the derivative $d\phi/d\xi$, we end up with the conservative form

$$\frac{d}{d\xi}\left\{\frac{a}{2}\left(\frac{d\phi}{d\xi}\right)^2 - W(\phi)\right\} = 0,$$

which can be integrated. Then, we infer

$$\frac{d\phi}{d\xi} = -\sqrt{\frac{2}{a}}\cdot\sqrt{W(\phi) - W(\phi_\pm)}, \tag{37}$$

recalling that ϕ is monotone decreasing since $\phi_+ < \phi_-$. Hence, among other solutions, equation (37) defines implicitly the steady profile $\phi = \phi(\xi)$ by

$$\int_{\phi(\xi_0)}^{\phi(\xi)} \frac{ds}{\sqrt{W(s) - W(\phi_\pm)}} = \sqrt{\frac{2}{a}}\,(\xi_0 - \xi)$$

connecting ϕ_- to ϕ_+ for any given $\xi_0 \in \mathbb{R}$. □

As an example, let us consider the case $f(u) = \kappa u(u-1/2)(1-u)$. Since the potential is given by $W(u) = \frac{1}{4}\kappa u^2(1-u)^2$, there holds

$$\int_{1/2}^{\phi(x)} \frac{2\,ds}{s(1-s)} = \sqrt{\frac{2\kappa}{a}}\,(x_0 - x)$$

that gives

$$\ln\left(\frac{\phi(x)}{1-\phi(x)}\right) = \sqrt{\frac{\kappa}{2a}}\,(x_0 - x).$$

Expliciting the value $\phi = \phi(x)$, we obtain

$$\phi(x) = \frac{1}{1 + e^{\sqrt{\frac{\kappa}{2a}}(x - x_0)}} \qquad (x_0 \in \mathbb{R}). \tag{38}$$

As stated at the beginning, the propagation speed is $c = 0$.

Third-order polynomial reaction function

Next, we focus on the case $c_\star > 0$, which occurs, again by formula (28), whenever $W(1) < W(0)$. In the cubic case

$$f(u) = \kappa u(u - \alpha)(1 - u) \tag{39}$$

with $\kappa > 0$, this translates into the choice $\alpha \in (0, 1/2)$.

To start with, let us focus on the limiting case $\sigma = \tau = 0$, that is on the parabolic reaction-diffusion equation

$$\partial_t u = a\,\partial_{xx} u + \kappa u(u - \alpha)(1 - u). \tag{40}$$

In such a case, there exist explicit formulas for both propagation speed c and front profile ϕ. Indeed, let us set

$$\frac{d\phi}{d\xi} = -A\phi(1 - \phi).$$

for some constant $A > 0$. Since

$$\frac{d^2\phi}{d\xi^2} = -A(1 - 2\phi)\frac{d\phi}{d\xi} = A^2\phi(1 - \phi)(1 - 2\phi),$$

inserting in (27) with $\sigma = \tau = 0$ and simplifying the factor $\phi(1 - \phi)$, we infer

$$(\kappa - 2aA^2)\phi + aA^2 - cA - \kappa\alpha = 0$$

which gives $A = \sqrt{\kappa/(2a)}$ and

$$c = c_0 := \sqrt{2a\kappa}\left(\tfrac{1}{2} - \alpha\right). \tag{41}$$

Thus, the corresponding profile ϕ solves the Bernoulli equation $d\phi/d\eta = -\phi + \phi^2$ where $\eta = (\kappa/2a)^{1/2}\,\xi$, which is explictly given by

$$\phi(\xi) = \frac{1}{1 + e^{\sqrt{\frac{\kappa}{2a}}(\xi - \xi_0)}} \qquad (\xi_0 \in \mathbb{R}),$$

which, incidentally, coincide with (38) when $\xi = x$.

When dealing with propagation fronts for (25) with $\sigma = 0$, that is

$$\tau\,\partial_{tt}u+\partial_t u=a\,\partial_{xx}u+f(u), \tag{42}$$

a formula, corresponding to (41), can be provided. Indeed, the equation (27) with $\sigma=0$ coincide with the traveling wave equation for (40) where a has been replaced by $a-\tau c^2$. Thus, adding the subscript τ to c to give evidence to dependency, there holds

$$c_\tau=\sqrt{2\,(a-\tau c_\tau^2)\kappa}\left(\tfrac{1}{2}-\alpha\right).$$

Squaring and rearranging, we infer

$$\left\{1+2\kappa\tau\left(\tfrac{1}{2}-\alpha\right)^2\right\}c_\tau^2=2a\kappa\left(\tfrac{1}{2}-\alpha\right)^2,$$

and thus

$$c_\tau=\frac{c_0}{\sqrt{1+\tau c_0^2/a^2}}. \tag{43}$$

where c_0 is given in (41). There is a strict connection between relation (43) and (34), being one the inverse of the other in the case $a=1$. Specifically, the relation (43) goes beyond the special case of the cubic f, holding for general reaction function. In particular, since $0\le c_\tau<c_0$ for $\tau>0$, as shown by the inequality

$$\frac{c_\tau-c_0}{c_0}=\frac{1}{\sqrt{1+\tau c_0^2/a^2}}-1<0,$$

the propagation phenomena is always slowed down when pure damping is added, inerta being limited to the deceleration effect of the front.

When dealing with hyperbolic reaction-diffusion equation (25) with $\sigma\in(0,\tau]$ and cubic f, to our knowledge, there is no available extension of the explicit formulas (41) and (43). In particular, as it will be shown later on, the addition of the relaxation term, i.e. $\sigma=\tau$, the situation is completely different in some regime of the parameter $\alpha\in(0,1)$.

Piecewise affine reaction function with a bistable shape

Finally, following the approach in [21], we compute explicit traveling wave solutions for a very specific form for the reaction function f of bistable type. Specifically, we concentrate on a piecewise affine function given by

$$f(u)=\begin{cases}-m\,u & u<\alpha,\\ m(1-u) & u\ge\alpha.\end{cases}\qquad m>0,\ \alpha\in(0,1), \tag{44}$$

(see Fig.2). In such a special case, it is possible to provide an explicit expression for both the traveling wave profile (ϕ,ψ) and of its speed c.

Let us go back to (35) and rewrite it as

$$\frac{d\phi}{d\xi} = \psi, \qquad (a-\tau c^2)\frac{d\psi}{d\xi} = m\,\phi - c\,(1+\sigma m)\,\psi, \tag{45}$$

to be matched at $\phi = \alpha$ with

$$\frac{d\phi}{d\xi} = \psi, \qquad (a-\tau c^2)\frac{d\psi}{d\xi} = m(\phi-1) - c\,(1+\sigma m)\,\psi. \tag{46}$$

Since the two singular points are saddles, the matching amounts in choosing the critical value of the parameter c such that the unstable manifold of the singular point $(0,0)$ intersects, at $\phi = \alpha$, the stable manifold of $(1,0)$.

The directions of the unstable/stable manifolds are described by the eigenvectors of the corresponding linearized equation. Hence, denoted by $(\tilde{\phi}, \tilde{\psi})$ the perturbation of the equilbrium state $(\bar{\phi}, 0)$, they are given by the eigendirection of the matrix

$$\mathbf{A} := \begin{pmatrix} 0 & 1 \\ m/(a-\tau c^2) & -c(1+\sigma m)/(a-\tau c^2) \end{pmatrix}$$

In particular, this means that (ϕ, ψ) belongs to the unstable/stable manifold if and only if $\tilde{\psi} = \lambda_\pm \tilde{\phi}$, where $\lambda_\pm$ denote the (positive/negative) roots of the characteristic polynomial

$$p(\lambda) = \det(\mathbf{A} - \lambda\,\mathbf{I}) = \frac{1}{a-\tau c^2}\left\{(a-\tau c^2)\lambda^2 + c(1+\sigma m)\lambda - m\right\}.$$

Specifically, the explicit values for $\lambda_\pm$ are

$$p(\lambda_\pm) = 0 \qquad \Longleftrightarrow \qquad \lambda = \lambda_\pm := \frac{-c(1+\sigma m) \pm \sqrt{\Delta(c)}}{2(a-\tau c^2)}$$

where the discriminant Δ is

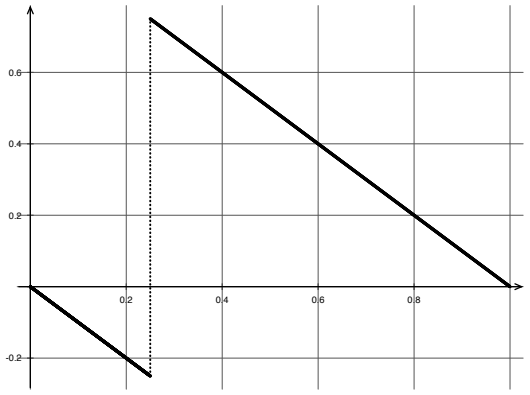

Fig. 2 Graph of the function f given in (44) with parameters $m = 1$ and $\alpha = 0.25$.

$$\begin{aligned}\Delta(c) &:= c^2(1+\sigma m)^2 + 4(a-\tau c^2)m \\ &= \left[(1-\sigma m)^2 - 4(\tau-\sigma)m\right] c^2 + 4am,\end{aligned}$$

which is strictly positive in the regime $c^2 < a/\tau$.

Thus, the stable manifold of $(0,0)$ and the unstable manifold at $(1,0)$ are respectively given by $\tilde{\psi} = \lambda_+ \tilde{\phi}$ and $\tilde{\psi} = \lambda_- \tilde{\phi}$, that is

$$\psi = \lambda_- \phi \qquad \text{and} \qquad \psi = \lambda_+(\phi - 1).$$

The two graphs intersect at $\phi = \alpha$ if and only if $|\lambda_-|\alpha = \lambda_+(1-\alpha)$. Recalling the explicit formulas for λ_- and λ_+, the latter equality can be rewritten as

$$\sqrt{\Delta(c_{\rm ex})}(1-2\alpha) = c_{\rm ex}(1+m\sigma).$$

After some straightforward algebraic manipulations, we end up with

$$c_{\rm ex} = \left\{ \frac{ma}{(1+m\sigma)^2\alpha(1-\alpha) + m\tau(2\alpha-1)^2} \right\}^{1/2} (1-2\alpha). \tag{47}$$

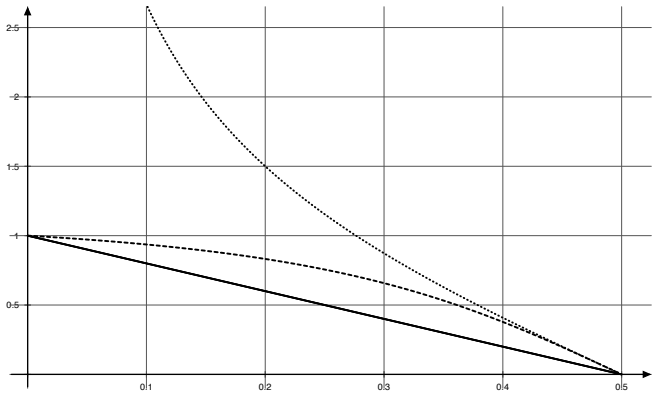

Fig. 3 Exact value of the speed, as in (47), with $a = m = 1$ and $\sigma = \tau = 0$ (dotted), $\sigma = 0$, $\tau = 1$ (dashed), $\sigma = \tau = 1$ (continuous).

Comparing the speeds $c_{\rm ex}$ for a generic choice of σ and τ and c_0 for $\sigma = \tau = 0$ gives

$$\frac{c_{\rm ex}}{c_0} = \left\{ \frac{\alpha(1-\alpha)}{(1+\sigma m)^2\alpha(1-\alpha) + \tau m(2\alpha-1)^2} \right\}^{1/2}$$

For $\sigma \in [0,\tau]$, since $\alpha(1-\alpha) < 1/4$ for $\alpha \neq 1/2$, there holds

$$\frac{\alpha(1-\alpha)}{(1+m\sigma)^2\alpha(1-\alpha)+m\tau(2\alpha-1)^2} < \frac{1}{(1+m\sigma)^2+4m\tau(2\alpha-1)^2} \leq 1$$

with the equality holding if and only if $\tau = 0$. hence, in the same regime, it follows

$$\frac{c_{\rm ex}-c_0}{c_0} = \left\{ \frac{\alpha(1-\alpha)}{(1+m\sigma)^2\alpha(1-\alpha)+m\tau(2\alpha-1)^2} \right\}^{1/2} - 1 < 0.$$

In particular, the (hyperbolic) propagation speed $c_{\rm ex}$ is always smaller than the corresponding (parabolic) speed c_0 for any choice of the couple σ and τ. This could be also recognised, observing directly that the value of $c_{\rm ex}$, regarded as a function of σ and τ, is strictly decreasing with respect to both variables.

Let us remark that, in such a case, the function f is discontinuous (increasing) at the value $u = \alpha$ and, thus, the first derivative of f is, lousely speaking, equal to $+\infty$. In particular, the dissipativity condition $1 - \sigma f' > 0$ is never satisfied at such a point whenever $\sigma > 0$, with dramatic consequences to be explored in the next Section.

3 Numerical computation of the propagation speed

From now on, we restrict the attention to two main cases corresponding to the choices: $\sigma = 0$, $\tau > 0$ and $\sigma = \tau > 0$, reported here for reader's convenience,

$$\begin{aligned} \tau\partial_{tt}u + \partial_t u &= a\partial_{xx}u + f(u) && \text{(damping)} \\ \tau\partial_{tt}u + \partial_t\{u - \tau f(u)\} &= a\partial_{xx}u + f(u) && \text{(relaxation)} \end{aligned}$$

where $f(u) = \kappa u(u-\alpha)(1-u)$ with $\kappa > 0$ and $\alpha \in (0,1)$. Coherently with the previous part of the paper, we focus on propagating waves connecting 1 at $-\infty$ with 0 at $+\infty$ in the case $\alpha \in (0, 1/2]$, so that the speed $c_{\rm ex}$ is non-negative as a consequence of the relation $W(1) \leq W(0)$, see identity (28).

3.1 Computation of the propagation speed

In the purely damped case, the explicit formula (43) for the propagation speed can be used to assess the reliability of the so-called *phase-plane algorithm*, presented in details in the next subsection. Differently, when relaxation is taken into account, there is no explicit formula for the velocity. Thus, an approximated version of its value should be considered as furnished by some algorithm. Based on the tests used on the damping case, we will consider as "exact" speed $c_{\rm ex}$ the ones provided by the phase-plane algorithm and use it to test the capability of two (dynamical) numerical schemes to provide reliable predictions.

Phase plane algorithm

As described in the paragraph *Local analysis* in Subsection 2.2, both the singular points of the ODE system for traveling waves are saddles and, as a consequence, both the corresponding unstable/stable manifold are one-dimensional. Therefore, the existence of a heteroclinic connection is equivalent to the fact that, for an appropriately tuned parameter $c = c_{\rm ex}$, the unstable curve exiting from the critical point $(1,0)$ intersects the stable curve entering the critical point $(0,0)$. Based on the rotated vector field property –see *Global analysis* in Subsection 2.2– we can perform a shooting-type argument and transform the problem of the existence of a heteroclinic traveling wave into the the search of a zero of a given function. Such step could be performed by preliminarly finding a reliable approximation to the solution of an ordinary differential equation and then by means of a standard interval division scheme, furnishing the exact value $c_{\rm ex}$ of the propagation speed.

To enter the details, we denote by $v_0 = v_0(\phi, c)$, the stable manifold of $(0,0)$ and by $v_1 = v_1(\phi, c)$ the unstable manifold of $(1,0)$. Then, we look for two different solution of the first order equation

$$\begin{aligned}\frac{\partial v}{\partial \phi} &= \frac{d\psi/d\xi}{d\phi/d\xi} \\ &= \frac{1}{a-\tau c^2}\left\{\frac{1}{\psi}\frac{dW}{du}(\phi) - c\left[1+\sigma\frac{d^2W}{du^2}(\phi)\right]\right\}\end{aligned}$$

with initial conditions along the stable/unstable manifold of $(0,0)/(0,1)$.

Curves v_0 and v_1 are determined approximately by choosing an initial datum on the corresponding stable/unstable manifold as provided by the linearized operator at the two critical points. Namely, at $\bar{u}$, we compute the eigenvectors relative to the eigenvalues $\lambda_\pm = \lambda_\pm(\bar{u}; c)$ as given by (32). Then, we compute the solutions $v_0 = v_0(\cdot, c)$ and $v_1 = v_1(\cdot, c)$ corresponding to the initial data

$$v_0(\theta, c) = \lambda_-(0,c)\theta \qquad \text{and} \qquad v_1(1-\theta, c) = -\lambda_+(1,c)(1-\theta)$$

for θ small enough and solving forward/backward (3.1) for v_0/v_1, respectively.

Next, we evaluate the difference function h of the solutions v_0 and v_1 at $u = \alpha$,

$$h(c) := v_0(\alpha, c) - v_1(\alpha, c),$$

for $c \in (-\sqrt{a/\tau}, \sqrt{a/\tau})$. It can be readily seen that

$$h(-\sqrt{a/\tau}) < 0 < h(\sqrt{a/\tau}).$$

Moreover, thanks to the rotated vector field property, the function h is strictly increasing in $(-\sqrt{a/\tau}, \sqrt{a/\tau})$ and, thus, it has a single zero, corresponding to the value $c_{\rm ex}$. The heteroclinic orbit corresponds to such a choice of the critical speed $c_{\rm ex}$ such that $h(c_{\rm ex}) = 0$, which is uniquely determined since the function h is strictly monotone increasing,

Heuristic validation of the phase-plane algorithm in the purely damped case

Next, we compare the exact formula (43) in the case $\sigma = 0$, $a = \kappa = 1$, recalled here for reader's convenience, viz.

$$c_{\rm ex} = \frac{\sqrt{2}\,(1/2-\alpha)}{\sqrt{1+2\tau\,(1/2-\alpha)^2}},$$

with the approximated value $c_{\rm du}$ provided by the phase-plane algorithm using the value $E_{\rm du}$ as measure of the relative error, defined by

$$E_{\rm du} := \left| \frac{c_{\rm du} - c_{\rm ex}}{c_{\rm ex}} \right| \tag{48}$$

To start with, we learn from Fig.4 that there is numerical evidence of a scheme of order 1 in the case $\tau = 1$. Different values of τ, a and κ fits into the same scenery.

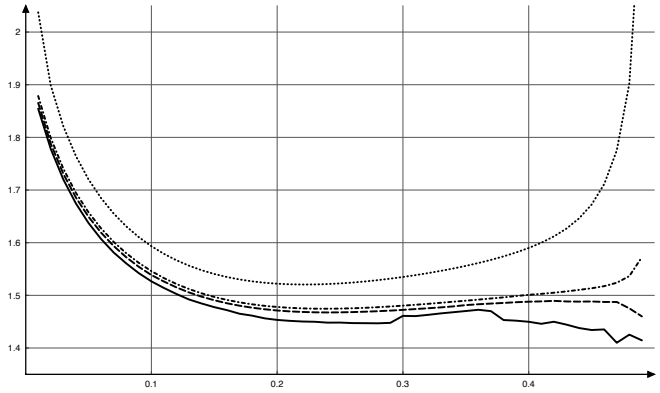

Fig. 4 Case $\tau = a = \kappa = 1$: graphs of the values of $E_{\rm du}/{\rm du}$ as a function of $\alpha \in (0, 0.5)$ where the relative error $E_{\rm du}$ is given in (48) for $\theta = 10^{-8}$ and discretization step equal to different choices of du: 10^{-2} (dotted), 10^{-3} (dotted-dashed), 10^{-4} (dashed), 10^{-5} (continuous).

From this, we extrapolate the final (reliable) choices ${\rm du} = 10^{-5}$ and $\theta = 10^{-8}$. The corresponding values for the exact formula $c_{\rm ex}$, the approximated value $c_{\rm du}$ and the relative error $E_{\rm du}$, are reported in Table 1, for different values of the unstable zero α, chosen as a value in $(0, 1/2)$.

In the case $\sigma \in (0, \tau]$ for some $\tau > 0$, to our knowledge, there is no explicit formula for the case of the double-well potential W, as in (26). Hence, we are forced to use an appropriate approximation of the speed as provided by the phase-plane algorithm with the values for du and θ previously detected. From now on, for simplicity, we will denote $c_{\rm du}$ by $c_{\rm ex}$ and consider the relative errors with respect to such an approximated value.

Table 1 Case $\tau = a = \kappa = 1$: values for c_{ex}, c_{du} and E_{du} relative to nine different choices of the unstable zero α relative to the choices $\text{du} = 10^{-5}$ and $\theta = 10^{-8}$.

α	c_{ex}	c_{du}	E_{du}
0.05	0.5368950	0.5369038	1.64×10^{-5}
0.10	0.4923660	0.4436135	1.53×10^{-5}
0.15	0.4436070	0.4436135	1.48×10^{-5}
0.20	0.3905667	0.3905724	1.45×10^{-5}
0.25	0.3333333	0.3333382	1.45×10^{-5}
0.30	0.2721655	0.2721695	1.46×10^{-5}
0.35	0.2075143	0.2075174	1.47×10^{-5}
0.40	0.1400280	0.1400300	1.45×10^{-5}
0.45	0.0705346	0.0705356	1.43×10^{-5}

To conclude, in Figure 5, we compare the values for the Allen–Cahn equation in the standard parabolic case, in the hyerbolic case with damping, in the hyperbolic case with relaxation. It is transparent that the role played in the latter is crucially different and it exhibits values α where the role of inertia is purely dissipative and others values for which sustained propagation is present.

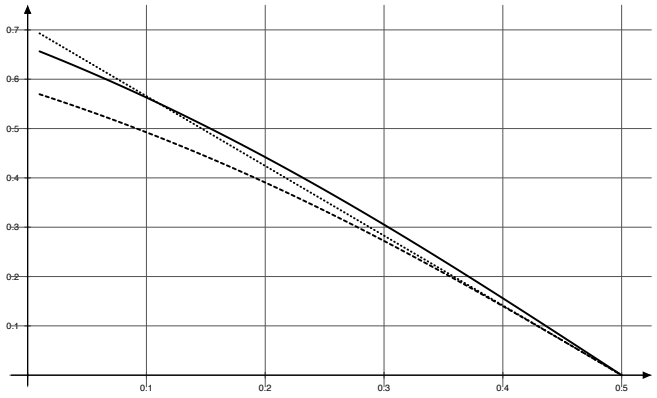

Fig. 5 Case $\tau = a = \kappa = 1$: comparison of the graphs of the speeds: parabolic Allen–Cahn (dotted), see (41)); hyperbolic Allen–Cahn with damping (dashed), see (43)); hyperbolic Allen–Cahn with relaxation (continuous).

3.2 PDE-based algorithms to approximate the propagation speed

The aim of this Subsection is to compare the capability of two different PDE-based algorithms to recover the speed of a propagation front. The strategy is different with respect to the one presented in Subsection 3.1, being of *dynamical* nature, i.e. grounded on the preliminary determination of the numerical solution of the underlying differential equation. Entering the details, we choose a scheme for the PDE and solve it in the space interval $[0,L]$, with zero-flux boundary conditions, in the time span $[0,T]$, corresponding to some initial datum.

Then, choosing two consecutive frames $u(\cdot,s)$ and $u(\cdot,t)$ with $0<s<t$, we look for a strategy furnishing a scalar value c such that

$$u(x,t)-u(y,s)\approx\phi(x-ct)-\phi(y-cs).$$

The key point stems in reducing from two functions (i.e. the solution profiles) to a single scalar value which should be able to describe, in principle, the overall propagating characteristic of the solution.

As numerical schemes, we consider the three approaches described in Subsection 1.3 (with the kinetic algorithm limited to the relaxation case), freezing the data relative to the two profiles $u(\cdot,s)$ and $u(\cdot,t)$ with $0<s<t$ appropriately chosen, and then determine an approximation of the propagation speed by means of some appropriately chosen algorithm.

Two main tools can be used to provide an approximation of the propagation speed, the *scout & spot algorithm* and the *LeVeque–Yee formula*, which we present in details in the following paragraphs.

Scout & spot algorithm

The first determines the speed of propagation considering a fixed level curve, say θ, taking into account the fact that, whenever the solution u converges to the propagating front ϕ, the relation $u(x,t)\approx\phi(x-ct)$ holds asymptotically in time, i.e. as $t\to+\infty$. Let $\phi_-<\phi_+$ and fix a value $\theta\in(\phi_-,\phi_+)$ and consider two different time instants, denoted here by t and s, such that $u(x(s),s)=u(x(t),t)=\theta$, then

$$x(t)-ct\approx\phi^{-1}(\theta)\approx x(s)-cs.$$

Hence, we deduce the approximation formula

$$c\approx\frac{x(t)-x(s)}{t-s}. \tag{49}$$

Translating such approximated rule in a definite algorithm is based on the introduction of a specific space mesh $J=\{x_1,\dots,x_j\}=\{\mathrm{dx},2\mathrm{dx},\dots,j\mathrm{dx}\}$. Assuming that the profile u_j^n is strictly monotone increasing with respect to j, the first step consists in considering the first value where the threshold θ is trespassed for any given time t^n, that is

$$n \longmapsto j^n(\theta) := \max\{j \in J : u_j^n < \theta\}.$$

Approximation formula (49) becomes

$$\begin{aligned} c_{\mathrm{s\&s}}^{n,p} = c_{\mathrm{s\&s}}^{n,p}(\theta) &= \frac{j^{n+p}(\theta) - j^n(\theta)}{t^{n+p} - t^n} \cdot \mathrm{dx} \\ &= \left[j^{n+p}(\theta) - j^n(\theta)\right] \cdot \frac{\mathrm{dx}}{p\,\mathrm{dt}} \end{aligned} \tag{50}$$

Such procedure corresponds to a *piecewise constant interpolation* of the states u_j^n and u_{j+1}^n. Moreover, the above formula shows that the propagation speed of slow waves provided by such a level curve algorithm is "quantized", that is any candidate as limiting speed is an *integer* multiple of the positive value by $\mathrm{dx}/(p\,\mathrm{dt})$.

Applying such an algorithm requires a number of choices, which can be matter of criticism, starting from the fact that the profile is expected to be monotone increasing. Here, we choose $\theta = \alpha$, $p = T/(2\mathrm{dt})$ so that the speed is approximated up to an error of order $\mathrm{dx}/(p\,\mathrm{dt}) = 10^{-2}$ in the case $T = 50$ and $\mathrm{dx} = 10^{-1}$.

LeVeque–Yee formula

The second strategy, inspired by [20], makes use of a spatial average of the profile and it does not require any monotone assumption on the solution. Anyway, it is still needed that the two asymptotic states, ϕ_- at $-\infty$ and ϕ_+ at $+\infty$, are different, i.e. the connection has to be heteroclinic.

Let ϕ be a differentiable function with asymptotic states $\phi(\pm\infty) = \phi_\pm$. The LeVeque–Yee formula takes advantage from the exact relation

$$\int_{\mathbb{R}} \{\phi(x+h) - \phi(x)\}\, dx = h\,[\phi]$$

where $[\phi] := \phi_+ - \phi_-$. The above formula can be proved by observing that

$$\begin{aligned} \int_{\mathbb{R}} \{\phi(x+h) - \phi(x)\}\, dx &= h \int_{\mathbb{R}} \int_0^1 \frac{d\phi}{dx}(x+\theta h)\, d\theta\, dx \\ &= h \int_0^1 \int_{\mathbb{R}} \frac{d\phi}{dx}(x+\theta h)\, dx\, d\theta \\ &= h \int_{\mathbb{R}} \frac{d\phi}{dx}(x+\theta h)\, dx = h\,[\phi]\,. \end{aligned}$$

Considering h equal to $-c\,\mathrm{dt}$ and assuming $[\phi] \neq 0$, the equality becomes

$$c = \frac{1}{[\phi]\,\mathrm{dt}} \int_{\mathbb{R}} \{\phi(x) - \phi(x - ct)\}\, dx.$$

Assuming that u_j^n is an approximation of $\phi(x_j - ct^n)$, we infer the estimate

$$c \approx c_{\mathrm{LY}}^{n,1} := \frac{\mathbf{1}\cdot(u^n - u^{n+1})}{[\phi]} \cdot \frac{\mathrm{dx}}{\mathrm{dt}} = \frac{1}{[\phi]} \sum_j (u_j^n - u_j^{n+1}) \cdot \frac{\mathrm{dx}}{\mathrm{dt}}, \tag{51}$$

where $\mathbf{1} = (1,\dots,1)$. The value c^n can be then considered as a space averaged propagation speed, which stabilizes when the approximation u^n converges to the given profile ϕ with constant velocity c.

3.3 Numerical experiments

Next, we intend here to compare the results produced by the two algorithms. In this respect, we have to specify the initial datum which will be chosen in the class of Riemann type, i.e. corresponding to the discontinuous function

$$u_0(x) = \begin{cases} 1 & x < 0, \\ 0 & x > 0, \end{cases}$$

with v_0 determined by the corresponding values obtained by setting $\partial_t u(x,0) = 0$ in the corresponding algorithm. Such choice is very natural, since we are looking for a solution converging to the traveling front connecting the two stable state.

We focus on the case of the cubic bistable nonlinearity $f(u) = \kappa u(u-\alpha)(1-u)$ with $\alpha \in (0,1)$, with the goal of matching the values for the velocity c_* as given by comparing the values provided by the exact formula (43) in the case $\sigma = 0$ and $\tau = 1$ and the value provided by the shooting argument, as described in Subsection 3.1. For sakeness of simplicity, we limit ourselves to the case $a = \kappa = 1$.

We numerically solve the corresponding PDE in the space interval $[0,L]$ –with zero-flux boundary conditions– in the time span $[0,T]$, where we consider the case $L = 50$, $T = 20$ with spatial mesh $\mathrm{dx} = 10^{-1}$ and time discretization $\mathrm{dt} = 10^{-3}$.

Finally, to quantify the error of the estimates we use the standard quantity

$$E_* := \left| \frac{c_*^{n,p} - c_{\mathrm{ex}}}{c_{\mathrm{ex}}} \right|,$$

where $* \in \{\mathrm{s\&s}, \mathrm{LY}\}$ and $p = 1$ if $* = \mathrm{LY}$.

Allen–Cahn equation with damping

In this part, we compare the exact formula for the propagation speed (43) with the approximated estimates obtained by applying in series one of the two scheme (first-order and Liénard) and, after that, the scout&spot algorithm (50) and the LeVeque–Yee formula (51). The results are summarized in Table 2, relatively to three different choices of the intermediate (unstable) zero α.

Table 2 Allen–Cahn equation with damping and polynomial reaction function, see (39): values of α and $c_{\rm ex} = c_{\rm ex}(\alpha)$, together with the different numerical scheme, corresponding speed estimates and relative errors.

α	$c_{\rm ex} = c_{\rm ex}(\alpha)$	*scheme*	s&s	$E_{\rm s\&s}$	LY	$E_{\rm LY}$
0.125	0.4685213	first-order	0.47	3.16×10^{-3}	0.4682076	6.69×10^{-4}
		Liénard	0.46	1.82×10^{-2}	0.4662342	4.88×10^{-3}
0.250	0.3333333	first-order	0.34	2.00×10^{-2}	0.3331151	6.55×10^{-4}
		Liénard	0.33	1.00×10^{-2}	0.3310495	6.85×10^{-3}
0.375	0.1740777	first-order	0.17	2.34×10^{-2}	0.1739747	5.92×10^{-4}
		Liénard	0.17	2.34×10^{-2}	0.1715496	1.45×10^{-3}

It is transparent the higher precision of the LeVeque–Yee formula (51) which add to the number of free parameters to be chosen in the scout&spot algorithm (such as the level θ, the value of p...), making the use of the latter strategy less effective.

Next, we pass to analyze the Allen–Cahn equation with a piecewise linear reaction function with a jump point located at $u = \alpha$. In this case, the crucial problem is, of course, the presence of a discontinuity in the source term. Thus, we compare the capability of the scout&spot algorithm and the LeVeque–Yee formula. The results, obtained by using the same numerical data previously described, are reported in Table 3. As can be appreciated from the values, the error is always of the order of 1%, which is largely acceptable.

Table 3 Allen–Cahn equation with damping and piecewise affine reaction function, see (44): Values of α and $c_{\rm ex} = c_{\rm ex}(\alpha)$, together with the different numerical scheme, corresponding speed estimates and relative errors.

α	$c_{\rm ex} = c_{\rm ex}(\alpha)$	*scheme*	s&s	$E_{\rm s\&s}$	LY	$E_{\rm LY}$
0.125	0.9149914	first-order	0.90	1.64×10^{-2}	0.9021793	1.40×10^{-2}
		Liénard	0.90	1.64×10^{-2}	0.9006799	1.56×10^{-2}
0.250	0.7559289	first-order	0.74	2.11×10^{-2}	0.7496325	8.33×10^{-3}
		Liénard	0.74	2.11×10^{-2}	0.7484820	9.85×10^{-3}
0.375	0.4588315	first-order	0.45	1.92×10^{-2}	0.4557922	6.62×10^{-3}
		Liénard	0.46	2.55×10^{-3}	0.4554450	7.38×10^{-3}

As shown by the numerical results, also the case of a discontinuous reaction function can be handled by both algorithms, with better error estimates for the LeVeque–Yee formula (which is also very easy to implement).

Allen–Cahn equation with relaxation

Finally, we consider the case of the hyperbolic Allen–Cahn equation with relaxation, that is (25) with $\sigma = \tau > 0$ (fixed equal to 1, for simplicity) for the third order polynomial reaction function, given by (39). In such a case, in addition to the first-order and Liénard schemes, we may also apply the kinetic scheme, also presented in Subsection 1.3. A selection of the results are collected in Table 4 and confirm the same conclusion as above: with the same space-time grid, the LeVeque-Yee formula is to be preferred, since it guarantees greater precision in speed approximation.

Table 4 Values of α and $c_{\mathrm{ex}} = c_{\mathrm{ex}}(\alpha)$, together with the different numerical schemes, speed estimates and relative errors.

α	$c_{\mathrm{ex}} = c_{\mathrm{ex}}(\alpha)$	*scheme*	s&s	$E_{\mathrm{s\&s}}$	LY	E_{LY}
0.125	0.5342843	first-order	0.53	8.02×10^{-3}	0.5335445	1.38×10^{-3}
		Liénard	0.53	8.02×10^{-3}	0.5318317	4.59×10^{-3}
		kinetic	0.54	1.07×10^{-2}	0.5347508	8.73×10^{-4}
0.250	0.3754283	first-order	0.38	1.22×10^{-2}	0.3750573	9.88×10^{-4}
		Liénard	0.37	1.45×10^{-2}	0.3728276	6.93×10^{-3}
		kinetic	0.38	1.22×10^{-2}	0.3758528	1.13×10^{-3}
0.375	0.1941490	first-order	0.19	2.14×10^{-2}	0.1940086	7.23×10^{-4}
		Liénard	0.19	2.14×10^{-2}	0.1913620	1.44×10^{-3}
		kinetic	0.19	2.14×10^{-2}	0.1943773	1.18×10^{-3}

Other numerical experiments have been performed with different choices of p and better precision for the estimate of the scout&spot algorithm, providing a corrisponding higher order of precision of the LeVeque–Yee formula, which appear again as a more precise tool. Comparing the three types of scheme –first-order reduction, Liénard, kinetic– the first two have some very poor resolution of the equation for short time, in particular when considered in relation with the third one. Spure oscillations are generated by both the schemes due to the presence of a discontinuity in the initial datum. Differently, the kinetic algorithm is capable of reproducing the correct behavior also in the short time (see [17, 18] for more numerical simulations). Nevertheless, we stress that the latter is much slower with respect to the other two. Thus, computing the propagation speed –which is a parameter relevant for the large-time behavior– the short time behavior is of secondary importance with respect to the capability of the scheme of being capable to reproduce the main features of the model in the long run, once the evolution has already solved the initial problem of the presence of a jump. This is particularly crucial because of the presence of the reaction term which, in large part of the space, pushes the solutions to stay close to stable solution of the underlying ODE.

The case of the piecewise affine reaction function, described in the last paragraph of Subsection 2.3, is harder to be simulated, since the numerical schemes of

Subsection 1.3 are not well-behaved in presence of discontinuos reaction function due to the presence of the term $\tau f(u)$ differentiated with respect to time. Numerical deficiencies arise already when performing simulations of the PDE, inherited by the jump of the reaction function f, probably due to the fact that the dissipativity condition $1 - \tau f' > 0$ is never satisfied at α whenever $\tau > 0$, At the moment, we are not aware of any numerical schemes which is capable of performing reliable simulations also in presence of discontinuities of the reaction function.

Acknowledgements Simulations have been performed by SCILAB 6.0.2, https://www.scilab.org/. R. G. Plaza was partially supported by DGAPA-UNAM, program PAPIIT, grant IN-100318.

References

1. Ali Y.M., Zhang L.C.; Relativistic heat conduction. International J. Heat Mass Transfer 48 (2005) 2397–2406.
2. Aronson D.G.; Weinberger H.F.; Multidimensional nonlinear diffusion arising in population genetics, Adv. in Math. 30 (1978), no. 1, 33–76.
3. Aronson D.G.; Weinberger H.F.; Nonlinear diffusion in population genetics, combustion, and nerve pulse propagation, in J.A. Goldstein "Partial differential equations and related topics", Lecture Notes in Mathematics, vol. 446, Springer Verlag (1975), 5–49.
4. Bouin E.; Calvez V.; Nadin G.; Hyperbolic traveling waves driven by growth. Math. Models Meth. Appl. Sci. 24, no.6 (2014) 1165–1195.
5. Cattaneo C.; Sulla conduzione del calore. Atti Sem. Fis. Univ. Modena 3 (1949) 83–101.
6. Cattaneo C.; Sur une forme de l'equation de la chaleur eliminant le paradoxe d'une propagation instantanée. C. R. Acad. Sci. Paris 247 (1958) 431–433.
7. Chester M.; Second sound in solids. Phys. Rev. 131, no.15 (1963) 2013–2015.
8. Christov C.I.; On frame indifferent formulation of the Maxwell-Cattaneo model of finite speed heat conduction, Mech. Res. Commun. 36 (2009) 481–486.
9. Cimmelli V.A.; Jou D.; Ruggeri T.; Ván P.; Entropy principle and recent results in non-equilibrium theories. Entropy 16 (2014) 1756–1807.
10. Courchamp F.; Berec L.; Gascoigne J.; "Allee effects in ecology and conservation". Oxford University Press, Oxford, 2008.
11. Criado-Sancho M.; Llebot J.E.; Behavior of entropy in hyperbolic heat conduction. Phys. Review E 47, no.6 (1993) 4104–4107.
12. Dreher M.; Quintanilla R.; Racke R.; Ill-posed problems in thermomechanics. Appl. Math. Letters 22 (2009) 1374–1379.
13. Hadeler K.P.; Rothe F.; Travelling fronts in nonlinear diffusion equations. J. Math. Biol. 2, no.3 (1975) 251–263.
14. Jordan P.M.; Dai W.; Mickens R.E.; A note on the delayed heat equation: Instability with respect to initial data. Mechanics Research Communications 35 (2008) 414–420.
15. Jou D.; Casas-Vàzquez J.; Lebon G.; Extended irreversible thermodynamics. Springer New York Dordrecht Heidelberg London, 4th edition, 2010.
16. Körner C.; Bergmann H.W.; The physical defects of the hyperbolic heat conduction equation. Appl. Phys. A 67 (1998) 397–401.
17. Lattanzio C.; Mascia C.; Plaza R.G.; Simeoni C.; Analytical and numerical investigation of traveling waves for the Allen–Cahn model with relaxation. Math. Models Meth. Appl. Sci. 26, no. 5 (2016) 931–985.
18. Lattanzio C.; Mascia C.; Plaza R.G.; Simeoni C.; Kinetic schemes for assessing stability of traveling fronts for the Allen–Cahn equation with relaxation. Appl. Numer. Math. 141 (2019) 234–247.

19. Lattanzio C.; Mascia C.; Plaza R.G.; Simeoni C.; Spectral stability of traveling fronts for nonlinear hyperbolic equations of bistable type *(this volume)*.
20. LeVeque R.J.; Yee H.C.; A study of numerical methods for hyperbolic conservation laws with stiff source terms. J. Comput. Phys. 86, no. 1 (1990) 187–210.
21. McKean H.P. Jr.; Nagumo's equation. Adv. Math. 4 (1970) 209–223.
22. Mitra K., Kumar S., Vedavarz S., Moallemi M.K.; Experimental evidence of hyperbolic heat conduction in processed meat. ASME J. Heat Transfer 117 (1995) 568–573.
23. Morse P.M.; Feshbach H.; Methods of theoretical physics. New York, NY: McGraw-Hill (1953).
24. Onsager L.; Reciprocal relations in irreversible processes I, Phys. Rev. 37 (1931), 405–426.
25. Vernotte P.; Les paradoxes de la théorie continue de l'équation de la chaleur. C. R. Acad. Sci. Paris 246 (1958) 3154–3155.